ELSEVIER

Physics of the Earth and Planetary Interiors 87 (1995) 231–246

PHYSICS
OF THE EARTH
AND PLANETARY
INTERIORS

Mantle anisotropy beneath the Tibetan Plateau: evidence from long-period surface waves

Yang Yu [a,*], Jeffrey Park [a], Francis Wu [b]

[a] *Department of Geology and Geophysics, Yale University, New Haven, CT 06520-8109, USA*
[b] *Department of Geological Sciences, SUNY, Binghamton, NY 13902-6000, USA*

Received 18 May 1994; accepted 24 June 1994

Abstract

We investigate long-period surface waves ($T > 100$ s) propagating across the Tibetan Plateau, based on the seismic records from a PASSCAL portable array and nearby Chinese Digital Seismic Network (CDSN) stations. Significant quasi-Love waveform anomalies, associated with fundamental Rayleigh–Love coupling, are consistently observed, suggesting that strong lateral gradients in azimuthal anisotropy exist beneath the plateau. More intense surface-wave scattering is observed at intermediate periods ($T \approx 50$ s), which suggests that the cause of the long-period quasi-Love waves lies in the upper mantle, not the thickened crust of the plateau. A detailed analysis of the data indicates that the long-period waveform anomalies are generated beneath the central Tibetan Plateau, where the structural trend implies deep deformations induced by continental collision. The absence of quasi-Love anomalies at the westernmost station of the Program for Array Seismic Studies of the Continental Lithosphere (PASSCAL) array suggests that the east–west extent of this mantle deformation is limited. Some, but not all, of the quasi-Love observations are consistent with SKS splitting observations. Both sets of observations predict a strong gradient in anisotropic properties in central Tibet. However, the quasi-Love waveforms are absent from records collected in the northern plateau for northerly propagation paths, which is not consistent with a gradient at the northern edge of the plateau, as suggested by SKS studies. This discrepancy indicates that the simple models used to interpret both body- and surface-wave data may be inadequate. Either significant P-wave anisotropy exists under the plateau, or the S-wave anisotropy does not possess a uniformly horizontal symmetry axis, or strong east–west gradients in anisotropy bias our data–synthetic comparison.

1. Introduction

Deformations involved in continent collision may cause lattice-preferred orientation of anisotropic minerals such as olivine and lead to a bulk elastic anisotropy in the upper mantle (Silver and Chan, 1991; Ribe, 1992). A study of seismic anisotropy can therefore help us understand better the deformation and evolution of the continental lithosphere. Previous seismic investigations in the Tibetan Plateau have not been able to address possible seismic anisotropy owing to the limitation in seismic data and on access to the region (see Molnar (1988) for a review). A passive

* Corresponding author.

SSDI 0031-9201(94)02971-7

PASSCAL (Program for Array Seismic Studies of the Continental Lithosphere) experiment has been carried out recently within the Tibetan Plateau using 11 portable broadband seismic stations (Owens et al., 1993). Shear-wave splitting from SKS phases shows evidence that a significant portion of the upper-mantle lithosphere beneath the Tibetan Plateau is strongly anisotropic (McNamara et al., 1994). SKS splitting as large as 2.4 s was reported, which would require an anisotropic layer nearly 300 km thick if S-wave anisotropy is limited to 4% variations. The magnitude and fast azimuth of S anisotropy inferred from SKS splitting also show strong lateral variation within the plateau and appear to be related to lithospheric deformation associated with the collision of India and Eurasia.

Surface waves propagating across the Tibetan Plateau will be strongly affected if significant seismic anisotropy exists in the crust, and particularly in the upper mantle. It is therefore important to investigate whether surface waves show evidence of mantle anisotropy beneath Tibet and what constraints on the structures can be obtained from them. Phase or group velocity tomography of surface waves has been used to study upper-mantle anisotropy at both global and regional scales (e.g. Nishimura and Forsyth, 1989; Montagner and Tanimoto, 1990, 1991; Wu and Levshin, 1994). However, the sparse path coverage and possible strong lateral variation in Tibet, as indicated by surface geology and SKS splitting, have made it very difficult to detect azimuthal-dependent velocity structure from phase or group velocity observations. Theoretical studies have shown that Rayleigh and Love surface waves interact in the presence of azimuthal anisotropy (Kirkwood and Crampin, 1981a,b; Kawasaki and Koketsu, 1990; Park, 1993), that is, elastic anisotropy with a horizontal axis of symmetry. Park

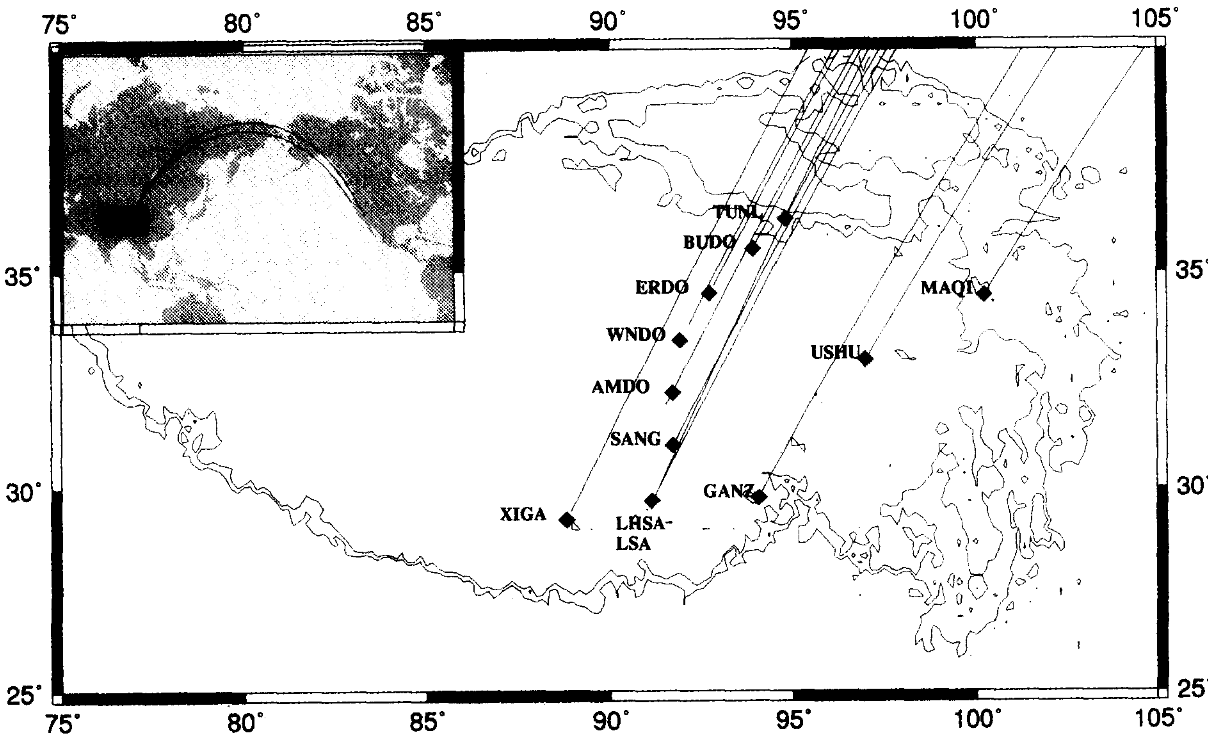

Fig. 1. Great circle paths (solid lines) for QL waveform observations within the Tibetan Plateau. Black diamonds and letters mark seismic station locations and names. The 3000 m and 4000 m contours of elevation are plotted to outline the Tibetan Plateau. The inset shows the surface-wave propagation paths outside Tibet (dark rectangle).

and Yu (1992, 1993) and Yu and Park (1993, 1994) demonstrated that significant waveform anomalies, associated with fundamental Rayleigh–Love coupling and termed 'quasi-Love' and 'quasi-Rayleigh' waves, can be generated in long-period ($T > 100$ s) seismic records by anisotropic upper-mantle structure. Fundamental-branch Rayleigh–Love coupling is particularly sensitive to lateral variations in azimuthal anisotropy, and the details of anomalous waveforms recorded at a single seismic station are determined by a horizontal integral of anisotropic properties along the wave path. Therefore, seismic waveforms recorded at a single station for a single event may give us valuable information about mantle anisotropy along the source–receiver great circle.

Tibet is a region with an apparent horizontal gradient in azimuthal anisotropy (McNamara et al., 1994) and where array measurement across this gradient zone can be made. It is therefore an ideal locale to gain further understanding of the generation of quasi-Love waves. We investigate long-period surface waves ($T > 100$ s) propagating across the Tibetan Plateau, based on the seismic records from a PASSCAL portable array and nearby Chinese Digital Seismic Network (CDSN) stations. Quasi-Love wave anomalies are consistently observed in the data, suggesting an anisotropic upper mantle beneath the Plateau. Using synthetic seismograms to model quasi-Love waves in anisotropic Earth models we find results that agree partially with SKS-splitting observa-

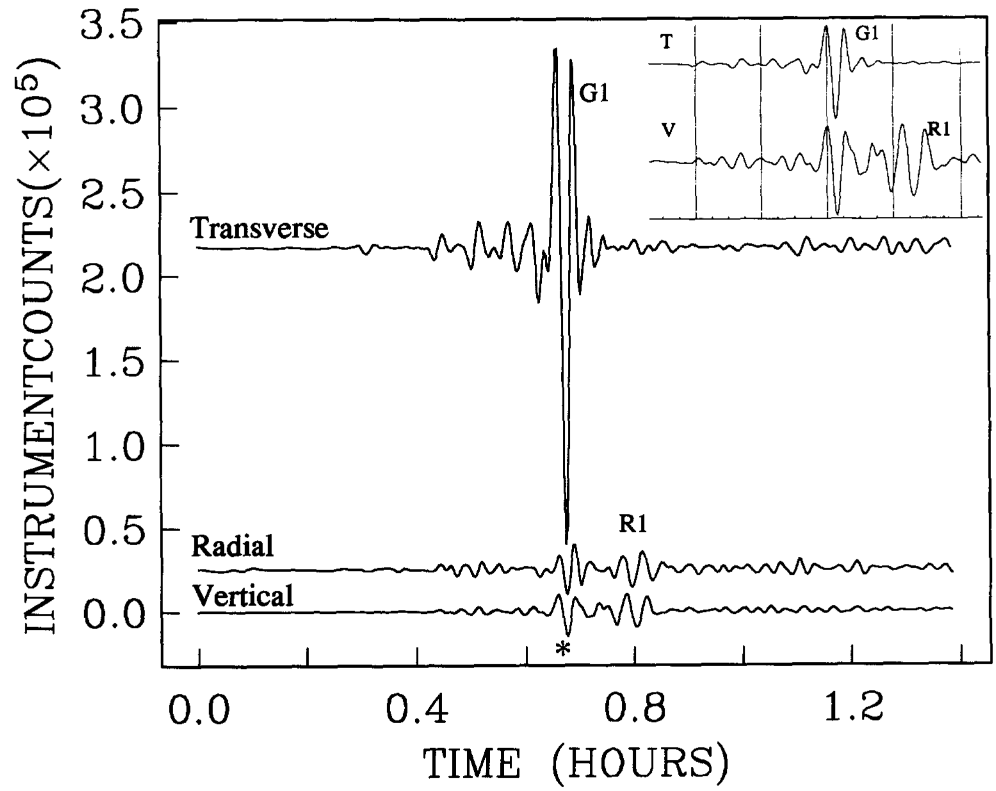

Fig. 2. VH-Channel seismic motion recorded at CDSN Station LSA after the 28 June 1992 $M_s = 7.5$ Landers earthquake in southern California. The data are lowpassed at 10 mHz. The horizontal components in the record were rotated to the transverse and radial components. G_1, The first wavepacket of the fundamental Love wave; R_1, the first wavepacket of the fundamental Rayleigh wave. The asterisk marks the QL waveform anomaly. Top panel shows in detail the phase relationship between Love wave on the transverse-component and QL wave on the vertical-component.

tions, which are determined by a vertical integral of anisotropic properties beneath individual seismic station, but that suggest further details of mantle deformation and elastic properties.

2. Data

We examined digital three-component long-period seismograms recorded at a permanent station of the CDSN and a passive PASSCAL deployment across the central Tibetan Plateau (Fig. 1). In 1 year of operation (July 1991–July 1992), 11 seismic stations with PASSCAL data logger and broadband STS-2 sensor (1/120 to 50 Hz) formed an array of 700 km length (Owens et al., 1993) which recorded many large earthquakes. For better observation of coupled Rayleigh and Love waves, we analyzed data from large, shallow, predominantly strike-slip events, with the observing stations near the Rayleigh source-radiation minima.

Fig. 2 shows seismic motion recorded at CDSN Station LSA after the 28 June 1992 $M_s = 7.5$ Landers earthquake of southern California, a strike-slip event with NEIC epicenter 34.18°N, 116.51°W, $d = 10$ km (Fig. 1). The strong waveform anomalies on the vertical- and radial-com-

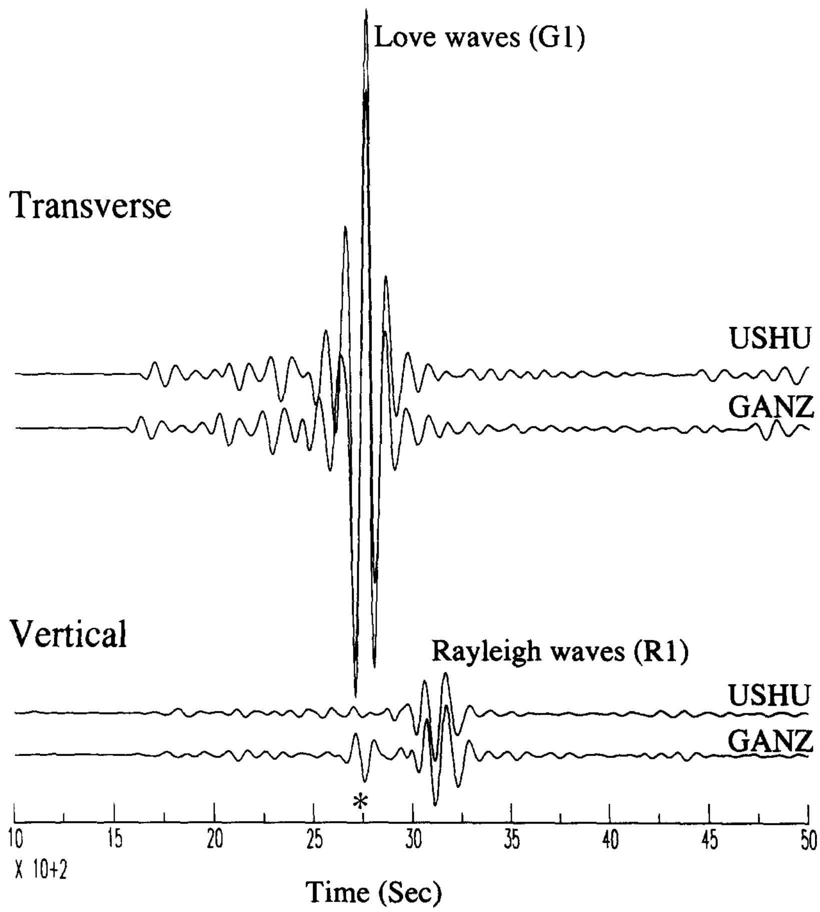

Fig. 3. Vertical- and transverse-component seismic data recorded at two PASSCAL stations, USHU and GANZ, for the 17 August 1991 $M_s = 7.1$ earthquake, off the northern California coast. The data are lowpassed at 10 mHz. The asterisk marks the QL waveform anomaly. There is no QL waveform anomaly at Station USHU. In contrast, a strong QL wave precursor to the Rayleigh wavepacket R_1 is evident at Station GANZ.

ponent records that arrive close to the Love wave G_1 and before the Rayleigh wave R_1 should be noted. We identify the anomalous waveform as a quasi-Love wave, a result of Rayleigh–Love coupling that transfers energy from transverse (Love) motion into radial–vertical (Rayleigh) motion. Strong quasi-Love waves suggest significant Rayleigh–Love coupling along the propagation path. However, the near-simultaneous arrival of a quasi-Love wave with the main Love wave (Fig. 2) suggests that Love-to-Rayleigh conversion takes place very close to the receiver LSA, which is located on the southern Tibetan Plateau. For several other large strike-slip earthquakes along the west coast of North America, similar quasi-Love waves are also observed at Station LSA.

Long-period seismic motions (lowpassed at 10 mHz) at two PASSCAL stations USHU and GANZ, are shown in Fig. 3. Surface waves generated by the 17 August 1991 $M_s = 7.1$ earthquake, off the northern California coast, when projected along a great circle path, arrived first at Station USHU and then at GANZ. Stations USHU and GANZ are within the Tibetan Plateau and only 400 km apart (see Fig. 1). The Love waves (G_1) and Rayleigh waves (R_1) are similar at the two stations. It should be noted that the seismic record at Station USHU, which is located at northeastern edge of the Tibetan Plateau, shows no quasi-Love wave on the vertical component, similar to a synthetic seismogram from a spherical Earth model. In contrast, a strong quasi-Love wave precursor to the Rayleigh wavepacket R_1 is evident on the vertical at Station GANZ, in the central–southern Plateau. Strong quasi-Love waves at Station GANZ, but not USHU, suggest that anomalous waveforms are generated by lateral structure somewhere between the two stations. This is confirmed by the phase relationship between main Love waves and quasi-Love waves at GANZ, which indicates that the quasi-Love wave is generated near GANZ. Seismic records for two other California events show similar waveform anomalies (Fig. 4). It should be noted that the

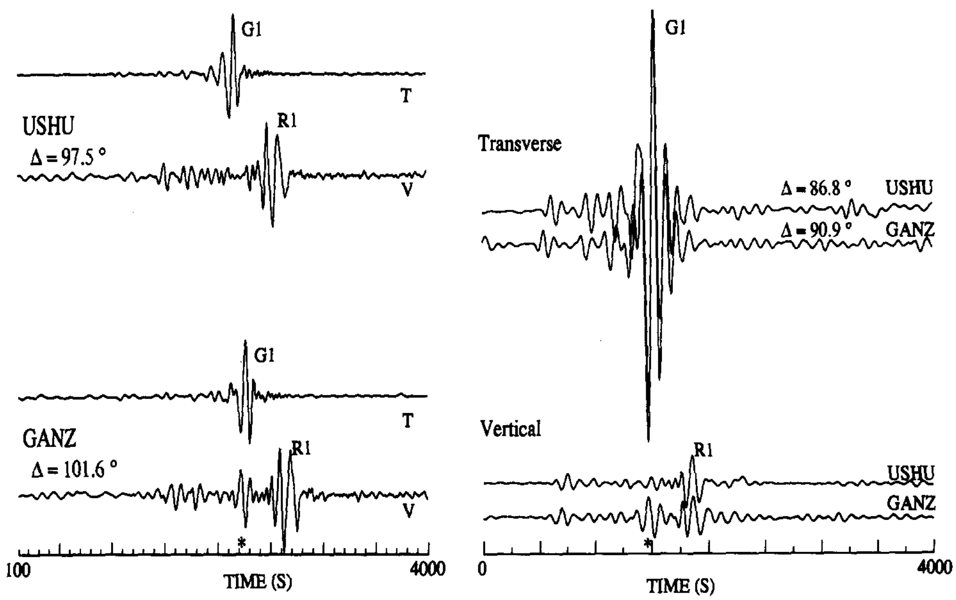

Fig. 4. Vertical- and transverse-component seismic data recorded at PASSCAL Stations USHU and GANZ for the 26 April 1992 $M_s = 6.7$ Northern California earthquake (left panel—the amplitudes are scaled for easy comparison) and the 6 April 1992 $M_s = 6.8$ Vancouver Island event (right panel). The data are lowpassed at 10 mHz. The asterisks mark the QL waveform anomalies. The epicenter distances (Δ) are also marked.

arrival time of QL waves, relative to the main Love waves (G_1), does not depend on the epicenter distance Δ.

It is instructive to examine surface waves that propagate along the north–south oriented PASSCAL array. Fortunately, seismic motions are well recorded at all PASSCAL stations for the 17 August 1991 earthquake off the northern California coast, so we can investigate how quasi-Love waves are developed within the Tibetan Plateau. Fig. 5 shows lowpassed (at 10 mHz) seismic motions along the array. Only vertical- and transverse-component seismic records are shown. In the Love-wave arrival window on the transverse component, vertical-component seismic records do not show significant quasi-Love-wave anomalies at Stations TUNL, BUDO, ERDO and WNDO, in the northern–central Plateau. However, a quasi-Love wave is apparent at Station AMDO, only 100 km south of WNDO in the central Plateau. Stronger quasi-Love waves appear further south on seismic records at Stations SANG and LHSA, in the central–southern Plateau. Similar features can be found in Fig. 6, which shows vertical seismic records along the array for another large earthquake near northern California. The data suggest that quasi-Love waves are generated in the central and southern Tibetan Plateau. We show in the next section that a strong lateral gradient in anisotropic properties between WNDO and AMDO, near the central Plateau, is consistent with the seismic data from the PASSCAL array.

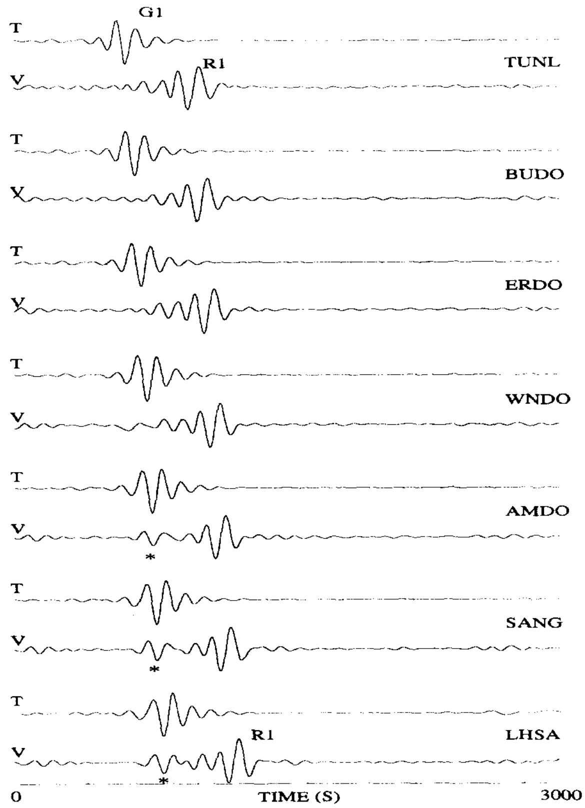

Fig. 5. Vertical- and transverse- component seismic motions along the north–south oriented PASSCAL array for the 17 August 1991 earthquake off the northern California coast. The data are lowpassed at 10 mHz, and the amplitudes are scaled for easy comparison. In the Love-wave (G_1) arrival time window, there is no significant QL wave anomaly at Stations TUNL, BUDO, ERDO and WNDO, in the northern–central Plateau. However, significant QL waves (marked by asterisks) appear at Stations AMDO, SANG and LHSA, in the central–southern Plateau.

3. Modeling

To understand better the upper-mantle structure responsible for the quasi-Love waveforms described above, we modeled long-period surface-wave propagation using anisotropic Earth models. We considered two upper-mantle models for the Tibetan Plateau. One model is based on the assumption that anisotropy is purely induced by mantle deformation involved in north–south compression associated with continental collision; the other is based on the results of SKS splitting observations.

In the first model (Fig. 7), an anisotropic perturbation zone was placed in a spherical reference Earth model (1066A, Gilbert and Dziewonski, 1975). The perturbed structure extends from 70 to 270 km depth in the upper mantle, roughly coincident with either a deep tectosphere or a shallow asthenosphere. For simplicity, we assume that the fractional velocity perturbation is constant with depth in the zone. The lateral variations occur within an anisotropic zone of 800 km width, comparable with the Tibetan Plateau. We assume S-wave anisotropy in the zone with an east–west horizontal fast symmetry axis (azimuthal anisotropy). The velocity anisotropy increases smoothly from zero to 4% at the center of the perturbation zone. The model is constructed to represent a possible anisotropic zone caused by north–south continent–continent collision. Crossing the collision zone, we expect a strong lateral variation in the level of mantle deformation and, of course, also in the magnitude of olivine lattice preferred orientation (LPO). We place the transition zone of deformation along the equator, for computational simplicity in our synthetic seismogram calculations. After comparing synthetic seismograms with the data, we can locate where the anisotropic gradient zone should be relative to the receivers. Synthetic seismograms across the anisotropic zone were calculated with the modal summation technique (Park and Yu, 1992; Yu and Park, 1993). We include the effects of Earth rotation and hydrostatic ellipticity in our modeling, but these have minor influence in this case.

Fig. 8 shows synthetic seismograms of $f < 10$ mHz, summed from the fundamental spheroidal and toroidal dispersion branches. The receiver is located at Site D in the center of the anisotropic zone (Fig. 7). As expected, there are significant waveform anomalies on the vertical and radial components before Rayleigh wavepacket R_1. The synthetic seismogram is similar to that observed at LHSA and GANZ (Figs. 2 and 3). Previous studies (Park and Yu, 1992, 1993; Yu and Park, 1993) demonstrated that anisotropy with a horizontal axis of symmetry generates these waveform anomalies more readily than lateral variations in isotropic S and P velocities, Earth topography, and anisotropy with a vertical axis of symmetry. Large quasi-Love waves, such as those observed in the data, are not produced by isotropic lateral structure consistent with global tomographic models of the mantle. In addition, we calculated synthetics for a similar zonal isotropic Earth model with a negative S-velocity perturbation of 6%, to model the influence of the shallow low-velocity zone in central Tibet (Molnar, 1988; Bourjot and Romanowicz, 1992; Zhao and Xie, 1993). The synthetic seismograms from this

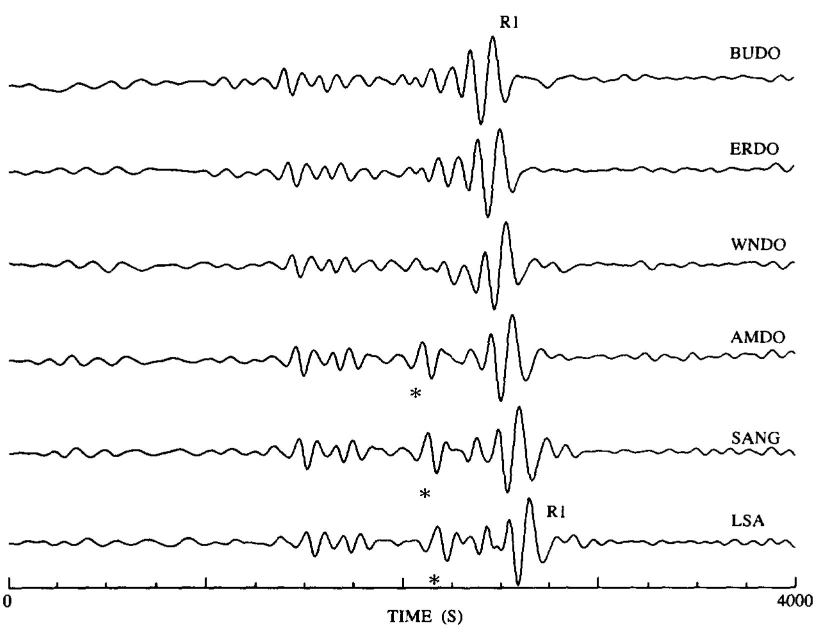

Fig. 6. Vertical-component seismic motions along the north–south oriented PASSCAL array for the 26 April 1992 Northern California earthquake. The data are lowpassed at 10 mHz. The asterisks mark the QL waveform anomalies.

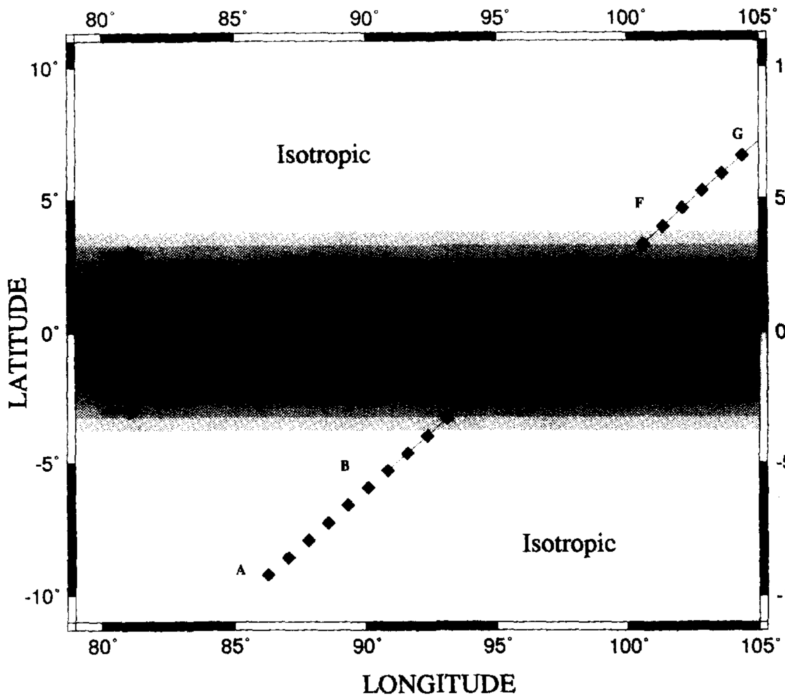

Fig. 7. Simple Earth model used in modeling the propagation of long-period surface waves in an anisotropic Earth. S-Wave velocities are perturbed in the shaded zone with lateral variations (0% at the edge, 4% at the center), in a layer from 70 to 270 km depth in the upper mantle. The black arrow shows the fast S-wave velocity direction. Squares and letters mark receiver locations. Also plotted are the great circle paths for which synthetic seismograms were constructed.

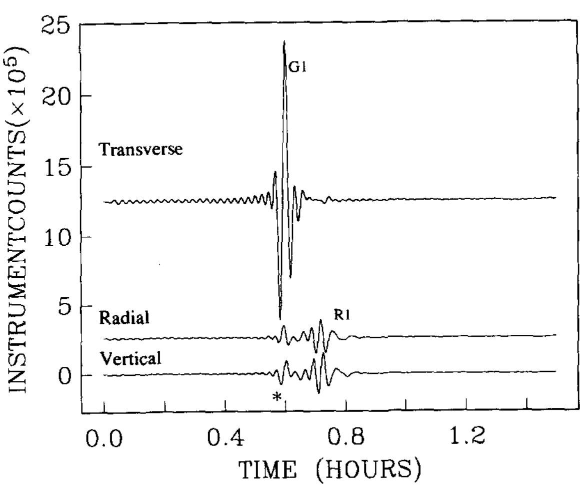

Fig. 8. Coupled-mode synthetic seismograms for the anisotropic Earth model shown in Fig. 7. The receiver is located in the anisotropic zone. The synthetics include all fundamental spheroidal and toroidal modes to $f = 10$ mHz. The asterisk marks the QL waveform anomaly.

isotropic Earth model do not show significant quasi-Love-wave anomalies with $f < 10$ mHz. To generate quasi-Love waves comparable with those observed in Tibet, anisotropy in the Earth's upper mantle is required in our modelings.

Comparing the quasi-Love waves in Fig. 8 with main Love waves on the transverse component, we find that they arrive nearly coherently, owing to Love-to-Rayleigh conversion near the receiver. Similar relationships are observed at Stations LSA (LHSA) and GANZ (Figs. 2 and 3). Fig. 9 shows how the quasi-Love-wave arrival time, relative to the main Love waves, is sensitive to the distance from the onset of the anisotropic gradient zone. Synthetics are calculated with a fixed source for Receivers D, C, B and A (Fig. 7). The quasi-Love wave recorded at Receiver D, which is located at the center of anisotropy zone, arrives close to the main Love waves. For Receiver C, 250 km further than Receiver D at the lower boundary of the anisotropic zone, the quasi-Love wave is delayed relative to the main Love wave because major

Love-to-Rayleigh conversion takes place a few hundred kilometers away from the receiver. Quasi-Love waves, after conversion from Love waves, travel with the slower Rayleigh wave group velocity. At receiver locations further south, at Sites B and A, the quasi-Love waves show a greater delay with the arrival of main Love wave G_1. In the data, we may well estimate where quasi-Love waves are generated using only a single seismic record. The likely uncertainty is less than 250 km in the frequency band we consider here, based on our modeling experiment. Tracing surface-wave propagations along a great circle path is another way to determine where quasi-Love wave are generated. Fig. 10 shows vertical synthetics for a number of receivers (from Site G

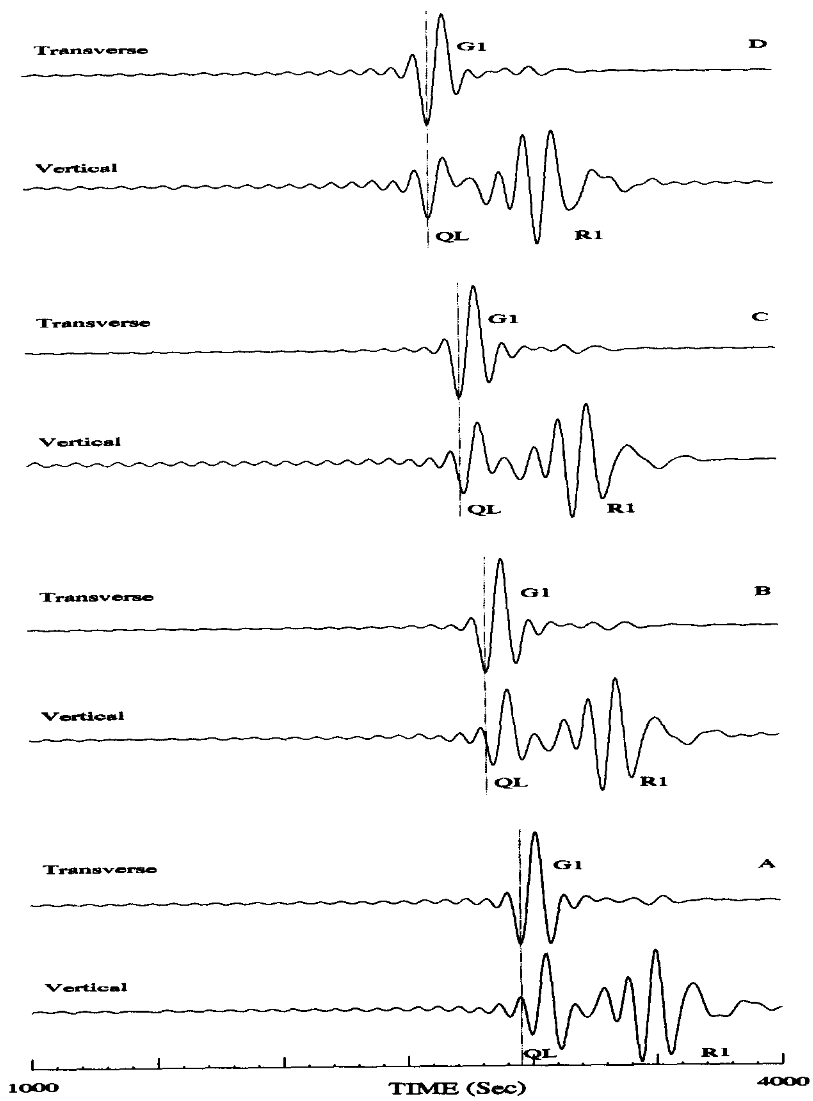

Fig. 9. Vertical- and transverse-component synthetic seismograms for the anisotropic Earth model shown in Fig. 7. For a fixed source, the synthetics are calculated for Receivers D, C, B and A along the same great circle path. The distance between receiver and center of the anisotropic zone increases as the receiver moves from D to A. (Note that QL wave arrival times, relative to the main Love waves, increase from D to A as well.)

to Site A in Fig. 7) along the same great circle path. Before the arrival of Rayleigh wavepacket R_1 we can find clearly a signal developing across the anisotropic zone. Weak long-period ($T \geqslant 250$ s) precursors to the Rayleigh wavepacket R_1 are caused by the mixed-type coupling induced by rotational Coriolis force (Park, 1986). Other than this, there is no significant quasi-Love wave at Receiver G, which is located far away from the anisotropic zone. A weak signal starts near Receiver F at the edge of the anisotropic zone. As the surface wave propagates across the perturbed zone, the quasi-Love waves become stronger. Significant waveform anomalies can be observed at all receivers beyond the anisotropic zone. Quasi-Love-wave observations at several stations along the same great circle path, such as along the PASSCAL array in Tibet, appear very useful for locating an anisotropic gradient zone.

Based on our modeling, we now can make a better estimate of where quasi-Love waves are generated in Tibet. In the eastern Plateau, following the path connecting USHU and GANZ, no waveform anomalies are observed at Station USHU, but strong quasi-Love waves are observed at GANZ. This suggests that quasi-Love waves observed at GANZ are generated somewhere between the two stations, most likely by a strong lateral gradient in anisotropic structure roughly 300 km north of GANZ. In the central Plateau, following a nearly north–south path connecting TUNL, BUDO, ERDO, WNDO, AMDO, SANG and LHSA, long-period surface-wave data for the 17 August 1991 northern California earthquake locate an anisotropic gradient between Stations WNDO and AMDO because significant quasi-Love-wave anomalies were observed only at Stations AMDO, SANG and LHSA. Combining with

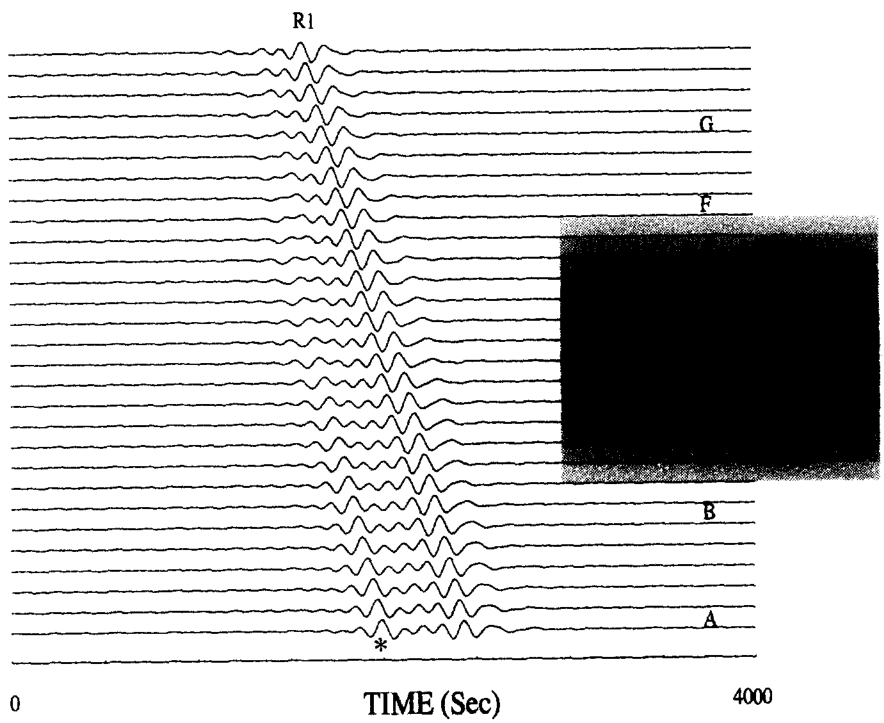

Fig. 10. QL waveform anomalies developed across an anisotropic gradient zone. Vertical synthetics are shown for a number of receivers (from Site G to Site A in Fig. 7) along the same great circle path. The shaded area marks the location of anisotropic gradient zone. (Note that the QL wave precursor to the Rayleigh wavepacket R_1 starts within the anisotropic zone.)

the observations along the USHU–GANZ path, we infer an anisotropic gradient zone in the central Tibetan Plateau (Fig. 11).

McNamara et al. (1994) analyzed SKS phases recorded at the PASSCAL array to determine the characteristics of shear-wave splitting in the upper mantle beneath the Tibetan Plateau, using 186 event–station pairs (Fig. 11). Delay times for SKS arrivals as large as 2.4 s are observed in the data, and argue strongly for an anisotropic upper mantle beneath the Plateau. Furthermore, measurements of the fast polarization direction and delay time for SKS arrivals reveal systematic variations along the north–south oriented PASSCAL array, suggesting strong lateral variations in anisotropic structure. In particular, substantial changes in the SKS delay time and fast direction occur across the gradient zone suggested by our surface-wave observations. The consistency of the results from quasi-Love waves and SKS splitting in Tibet are encouraging. To make a more detailed comparison, we constructed a 2-D anisotropic upper-mantle model for the Tibetan Plateau using the results from SKS splitting observations. The magnitude and fast direction of anisotropic structure along the north–south oriented PASSCAL array were interpolated with a cubic spline. As there are no SKS-splitting data available in the region away from the PASSCAL array, we have to make some assumptions. We first assume that the region north or south of the array is isotropic. The SKS splitting results then are interpreted as elastic variations within an anisotropic layer with a constant thickness (200 km). There are significant differences between observed data and the quasi-Love waves generated by the model

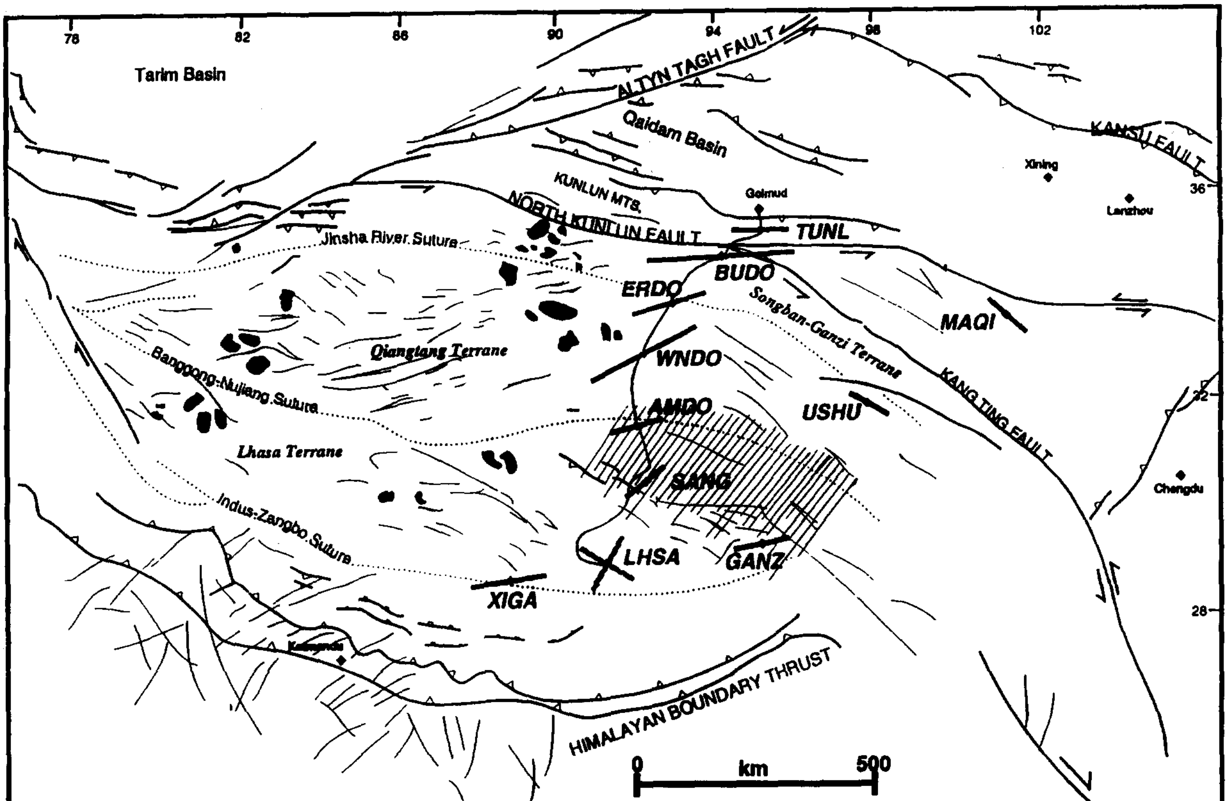

Fig. 11. A possible anisotropic gradient zone (shaded area) in the central Tibetan Plateau consistent with the QL wave observations. Also shown are major faults, sutures, terranes and the results from SKS splitting analyses (McNamara et al., 1994). The maps are modified from those plotted by Dewey et al. (1988) and McNamara et al. (1994).

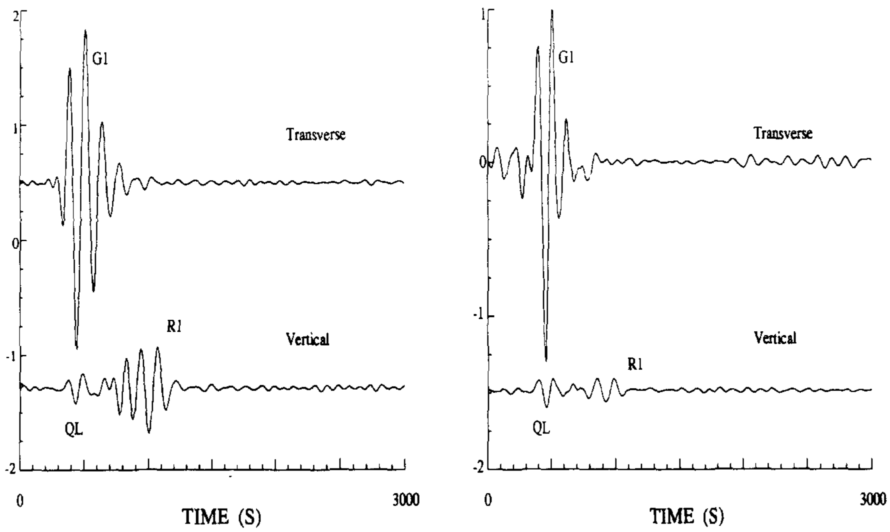

Fig. 12. Left panel: vertical- and transverse-component synthetic seismograms for an anisotropic Earth model. The model is based on the results from SKS splitting analysis (McNamara et al., 1994). The source-receiver geometry is identical to Landers-LSA. The CMT source solution was used, which misfits the amplitude of R_1 in this case. Right panel: long-period seismic data recorded at LSA for the 28 June 1992 Landers event. QL marks the quasi-Love waveform anomaly.

in coupled-mode synthetics with $f \leqslant 10$ mHz. First, the quasi-Love-wave anomalies in the synthetics are much weaker than those observed in the data. Second, the synthetic quasi-Love wave at LHSA (LSA) arrives significantly late relative to the Love wave because the strongest lateral gradient in the SKS model is located at the northern edge of the Plateau. Therefore, the as-

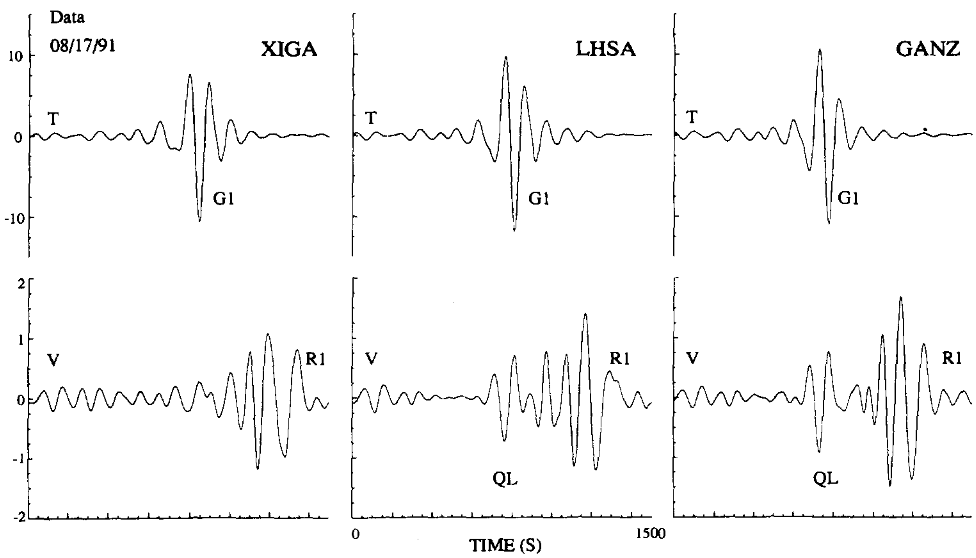

Fig. 13. Vertical- and transverse-component seismic data recorded at Stations GANZ, LHSA and XIGA for the 17 August 1991 earthquake, off the northern California coast. The data are lowpassed at 10 mHz, and the amplitudes are scaled for easy comparison. Strong QL waves are shown at GANZ and LHSA. There is only a very weak QL wave at XIGA.

sumption that there is no anisotropy beyond TUNL seems unlikely. We constructed an alternative model by using the fast direction of SKS splitting only, and assuming that the magnitude of azimuthal anisotropy is the same everywhere. In this model, the lateral gradient of anisotropic structure is caused by a rotation of the fast direction from 90° strike, in the region north of the PASSCAL array, to nearly 45° in the southern Plateau. The quasi-Love waves generated by this model appear able to explain our observations qualitatively (Fig. 12). However, the anisotropy prescribed by this model, especially the simplifications far from the stations, may not be realistic, and differs from the SKS results in detail.

Quasi-Love-wave anomalies in seismic records are affected by both S-wave and P-wave velocity anisotropy in the crust and mantle, unlike SKS splitting, which is interpreted in terms of only S-wave anisotropy. In our theoretical modelings, we consider only S-wave anisotropy, which may bias our inferences. P-Wave anisotropy beneath the Tibetan Plateau could shrink or enlarge the difference between the results from SKS splitting and quasi-Love-wave observations. Another shortcoming in our modelings is zonal (2-D) anisotropic structure, which is prescribed to make the calculations feasible; 2-D structure is not the case in the Tibetan Plateau, even approximately, as the PASSCAL data indicate strong east–west lateral variations (Fig. 13). Seismic records at the PASSCAL Station XIGA show only a weak quasi-Love anomaly for the 17 August 1991 event off northern California. XIGA is only 150 km west of Station LHSA, where strong quasi-Love waves are observed for the same event. At the easternmost station, GANZ, stronger QL waves are observed. This example demonstrates that we cannot always extend our inferences, as well as those from SKS splitting analyses, to regions not sampled directly by splitting and quasi-Love observations.

4. Discussion and conclusion

Significant quasi-Love-wave anomalies, associated with fundamental Rayleigh–Love coupling, are consistently observed at seismic stations in the central–southern Tibetan Plateau. More intense surface-wave scattering is observed at intermediate periods ($T \approx 50$ s), which suggests that the cause of the long-period quasi-Love waves ($T = 100$–250 s) lies in the upper mantle, not the thickened crust of the plateau. The Tibetan Plateau was created as a consequence of collision between the Indian and Eurasian continents. Seismic source mechanisms for events in and around the Plateau, topography and thrust faulting on the Plateau indicate compression in a direction orthogonal to the Himalayas. High-altitude mountain belts, large strike-slip faults, and major suture zones within the main part of the Plateau are all east–west trending, and indicate strong north–south deformation in the underlying upper mantle. Consequently, strong east–west preferred orientation of anisotropic crystals in peridotite should be produced in the upper mantle, leading to strong lateral variations of seismic velocity anisotropy beneath the central Plateau. The quasi-Love-wave observations, which are strongly correlated with surface geologic deformation fabrics, favor an anisotropic transition zone model in the central–south Plateau. Surface deformation features associated with the Tanggula Shan are consistent with the strong quasi-Love observations east of Lhasa. Speculatively, weak quasi-Love-wave generation in the western and northern Plateau may be due to the volcanism in that region. Arnaud et al. (1992) investigated the volcanism at the west and north of the Plateau, and concluded that the rocks are very similar to those produced by island-arc volcanism, which would occur if south-dipping subduction occurs at the northern edge of Tibet. Water released by a subducting slab would lower the melting temperature in the overlying mantle wedge, lower its seismic velocity, and could also inhibit the development of LPO anisotropy (Karato et al., 1986). Alternatively, temperature-related annealing may retard the development and retention of LPO.

Quasi-Love waveforms, however, are sensitive primarily to the gradient, not the absolute level of anisotropic properties. The surface-wave data can be satisfied by other models in which the anisotropic properties vary in different ways, for example, from polarization anisotropy (anisotropy with a vertical symmetry axis) to azimuthal anisotropy (anisotropy with a horizontal symmetry axis), or from a nearly east–west fast direction in azimuthal anisotropy to a NE direction, similar to the SKS-splitting in the central Plateau, or from anisotropic to isotropic along the path. In contrast to this multiplicity of possible models, a strong gradient in anisotropic properties at the northern edge of the Plateau, suggested by SKS splitting results, is not supported by our data. This discrepancy indicates that the simple models used to interpret both body- and surface-wave data may be inadequate. Possibly, significant P-wave anisotropy exists under the plateau, or the S-wave anisotropy does not possess a uniformly horizontal symmetry axis, or strong east–west gradients in anisotropy bias our data–synthetic comparison.

Low seismic velocities beneath the north–central Plateau, extremely low in some cases, have been reported by many seismic studies (Molnar and Chen, 1984; Brandon and Romanowicz, 1986; Molnar, 1990; Zhao et al., 1991), suggesting hot mantle. In particular, Ni and Baranzangi (1983) and Beghoul et al. (1993) identified in the northern–central Plateau an inefficient zone for S_n propagation, which was attributed to the partial melting of upper-mantle materials. A possible convective model with upwelling in north–central Tibet and downwelling in the surrounding region was proposed (Molnar, 1988, 1990). In support of this model, high heat flow and late Cenozoic volcanism are observed in north–central Tibet (e.g. Burke et al., 1974; Molnar et al., 1987). The vertical flow would produce strong polarization anisotropy, but very weak azimuthal anisotropy beneath north–central Tibet. This is consistent with our quasi-Love observations in the Tibetan Plateau because strong quasi-Love wave anomalies are observed only at stations in south–central Tibet. The strong anisotropic gradient zone in the central Tibetan Plateau suggested by quasi-Love wave anomalies is consistent with a change of fast velocity direction (approximate symmetry axis of mantle peridotites) from nearly vertical in north–central Tibet to horizontal in south–central Tibet. However, a straightforward interpretation of SKS splitting disagrees with the upward flow model, as it predicts a thick layer of azimuthal anisotropy in north–central Tibet. The interpretation of SKS splitting observations has not yet extended to cases where the symmetry axis is not horizontal, or to geometries where P-wave anisotropy can affect an incoming S wave.

Long-period surface-wave data show evidence that a significant portion of upper mantle beneath the Tibetan Plateau is anisotropic. However, details of mantle anisotropy, such as its magnitude and orientation, have not yet been well resolved. Most data we used are from seismic data recorded within Tibet for events along the west coast of North America. The data from several events but along similar paths help us confirm the existence of quasi-Love waves. However, such a data set makes it very difficult to infer the fast direction and magnitude of anisotropic structure because the strength of quasi-Love waves depends on not only the level of anisotropy but also the propagation azimuth relative to the fast or slow velocity direction. For example, no quasi-Love waves will be generated for a path along the fast or slow velocity direction of anisotropic structure (Yu and Park, 1993). Therefore, more data analysis and better path coverage are needed to improve our knowledge of upper-mantle anisotropy beneath Tibet.

The strong lateral variations in isotropic velocity structure or azimuthal anisotropy may lead to significant refractions of Love and Rayleigh waves in the horizontal plane (Woodhouse and Wong, 1986; Yu and Park, 1994). Some seismic records from the Tibetan Plateau show surface-wave refractions. For example, long-period Love waves recorded at Station XIGA for the events along the coast of North America show nearly 5° refraction to the west, consistent with refraction away from a low-velocity region in north-west Tibet. Therefore, the anisotropic gradients inferred from our surface-wave observations could have some uncertainties off the paths. As indicated by Park and Yu (1992), quasi-Love waves are strongly frequency dependent. Smoother deeper structure generates quasi-Love waves in longer periods.

That fact may help us constrain the depth of anisotropy, an unsolved problem for SKS analysis. However, in Tibet, it is more difficult to determine whether quasi-Love waves exist at periods $T < 100$ s because time-concentrated quasi-Love waves often become immersed in a scattered-wave coda as frequency increases. Clear quasi-Love waveforms in the period range $T =$ 100–250 s argue for anisotropic structure in the upper mantle rather than the crust.

Acknowledgments

We thank Paul Silver and D.E. McNamara for helpful discussions, and Lian-She Zhao for sending us preprints. The Chinese Digital Seismic Network is funded by the Advanced Research Projects Administration and maintained by the US Geological Survey. Tom Owens, George Randall, R. Zeng and their research groups are thanked for the quality of their field-work and the rapidity with which it was made available to their colleagues. US funding for the field experiment was provided by NSF Awards EAR-9004428, EAR-9005594 and EAR-9004221. This work was supported by NSF Grants EAR-9219367, EAR-9004220 and EAR-9206545, and Grant F49620-94-1-0043 of the US Air Force Office of Scientific Research, partly while J. Park was enjoying sabbatical leave at the Department of Terrestrial Magnetism, Carnegie Institute of Washington.

References

Arnaud, N.O., Vidal, Ph. P. Tapponnier Matte, Ph. and Deng, W.M., 1992. The high K_2O volcanism of northwestern Tibet: geochemistry and tectonic implications, Earth Planet. Sci. Lett., 111: 351–367.

Beghoul, N., Baranzangi, M. and Isacks, B.L. 1993. Lithospheric structure of Tibet and Western North America: mechanisms of uplift and a comparative study. J. Geophys. Res., 98: 1997–2016.

Bourjot, L. and Romanowicz, A., 1992. Crust and upper mantle tomography in Tibet using surface waves, Geophys. Res. Lett., 19: 881–884.

Brandon, C. and Romanowicz, A. 1986. A "NO-LID" zone in the central Chang-Thang platform of Tibet: evidence from pure path phase velocity measurements of long-period Rayleigh waves, J. Geophys. Res., 91: 6547–6564.

Burke, K.C., Dewey, J.F. and Kidd, W.S.F., 1974. The Tibetan Plateau: its significance for tectonics and petrology, Geol. Soc. Am. Abstr. Prog., 6: 1027–1028.

Dewey, J.F., Shackleton, R.M., Chang Cheng, F.R.S. and Yiyin, S., 1988. The tectonic evolution of the Tibetan Plateau, Philos. Trans. R. Soc. Lond., 327: 379–413.

Gilbert, F. and Dziewonski, A.M., 1975. An application of normal mode theory to the retrieval of structural parameters and source mechanisms from seismic spectra, Philos. Trans. R. Soc. Lond., Ser. A, 278: 187–269.

Karato, S., Paterson, M.S. and Gerald, J.D.F., 1986. Rheology of synthetic olivine aggregates: influence of grain-size and water, J. Geophys. Res., 91: 8515–8176.

Kawasaki, I. and Koketsu, K., 1990. Rayleigh–Love wave coupling in an azimuthally anisotropic medium. J. Phys. Earth, 38: 361–390.

Kirkwood, S. and Crampin, S., 1981a. Surface-wave propagation in an ocean basin with an anisotropic upper mantle: numerical modeling. Geophys. J. R. Astron. Soc., 64: 463–485.

Kirkwood, S. and Crampin, S., 1981b. Surface-wave propagation in an ocean basin with an anisotropic upper mantle: observations of polarization anomalies, Geophys. J. R. Astron. Soc., 64: 487–497.

McNamara, D.E., Owens, T.J., Silver, P.G. and Wu, F.T., 1994. Shear wave anisotropy beneath the Tibetan Plateau, J. Geophys. Res., 99: 13655–13665.

Molnar, P., 1988. A review of geophysical constraints on the deep structure of the Tibetan Plateau, the Himalaya and the Karakoram, and their tectonic implications, Trans. R. Soc. Lond., Sec A 327: 33–88.

Molnar, P., 1990. S-Wave residuals from earthquakes in the Tibetan region and lateral variations in the upper mantle. Earth Planet. Sci. Lett., 101: 68–77.

Molnar, P. and Chen, W.P., 1984. S–P travel time residuals and lateral inhomogeneity in the mantle beneath Tibet and the Himalaya, J. Geophys. Res., 89: 6911–6917.

Molnar, P., Burchfiel, B.C., Zhao, Z., Liang, K., Wang, S. and Huang, M., 1987. Geological evolution of northern Tibet: results of an expedition to Ulugh Muztagh, Science, 235: 299–305.

Montagner, J.-P. and Tanimoto, T., 1990. Global anisotropy in the upper mantle inferred from the regionalization of phase velocities, J. Geophys. Res., 95: 4797–4819.

Montagner, J.-P. and Tanimoto, T., 1991. Global upper mantle tomography of seismic velocities and anisotropies, J. Geophys. Res., 96: 20337–20351.

Ni, J. and Baranzangi, M., 1983. High frequency seismic wave propagation beneath the Indian shield, Himalayan arc, Tibetan Plateau and surrounding regions: high uppermost mantle velocities and efficient propagation beneath Tibet, Geophys. J. R. Astron. Soc., 72:665–689.

Nishimura, C.E. and Forsyth, D.W., 1989. The anisotropic structure of the upper mantle in the Pacific. Geophys. J., 96: 203–230.

Owens, T.J., Randall, G.Z., Wu, F.T. and Zeng, R., 1993. PASSCAL instrument performance during the Tibetan

Plateau passive seismic experiment. Bull. Seismol. Soc. Am., 83: 1959–1970.

Park, J., 1986. Synthetic seismograms from coupled free oscillations: the effects of lateral structure and rotation. J. Geophys. Res., 91: 6441–6464.

Park, J., 1993. The sensitivity of seismic free oscillations to upper mantle anisotropy, zonal symmetry. J. Geophys. Res., 98: 19933–19949.

Park, J. and Yu, Y., 1992. Anisotropy and coupled free oscillations: simplified models and surface wave observations. Geophys. J. Int., 110: 401–420.

Park, J. and Yu, Y., 1993. Seismic determination of elastic anisotropy and mantle flow, Science, 261: 1159–1162.

Ribe, N.M., 1992. On the relationship between seismic anisotropy and finite strain. J. Geophys. Res., 97: 8737–8748.

Silver, P.G. and Chan, W.W., 1988. Implications for continental structure and evolution from seismic anisotropy. Nature, 335: 34–39.

Woodhouse, J.H. and Wong, Y.K., 1986. Amplitude, phase and path anomalies of mantle waves. Geophys. J. R. Astron. Soc., 87: 753–774.

Wu, F.T. and Levshin, A.L., 1994. Group velocity tomography of East Asia. Phys. Earth Planet. Inter, 84: 59–77.

Yu, Y. and Park, J., 1993. Upper mantle anisotropy and coupled-mode long-period surface waves. Geophys. J. Int., 114: 473–489.

Yu, Y. and Park, J., 1994. Hunting for azimuthal anisotropy beneath the Pacific Ocean region. J. Geophys. Res., 99: 15399–15421.

Zhao, L.S. and Xie, J., 1993. Lateral variations in compressional velocities beneath the Tibetan Plateau from Pn traveltime tomography. Geophys. J. Int., 115, 1070–1084.

Zhao, L.S., Helmberger, D.V. and Harkrider, D.G., 1991. Shear-velocity structure of the crust and upper mantle beneath Tibetan and southeastern China. Geophys. J. Int., 105: 713–730.